DEFORMATION OF THE ARCTIC OCEAN SEA ICE COVER BETWEEN NOVEMBER 1996 AND APRIL 1997: A SURVEY

Ronald Kwok

Jet Propulsion Laboratory
California Institute of Technology
4800 Oak Grove Dr
Pasadena, CA 91109

Abstract

Quasi-linear features of the scale of kilometers to hundreds of kilometers can be observed in the high-resolution deformation fields of the sea ice cover produced by the RADARSAT Geophysical Processor System. They appear as sharp discontinuities separating regions of uniform ice motion. These features are expressions of one of five kinematic processes: opening, closing, shear, shear with closing, and shear with opening. Here, we refer to them as linear kinematic features (LKFs). Open water is created during an opening event and ridges are formed during a closing event. Shear, however, does not always result in convergence or divergence that modify the sea ice thickness distribution. The character of the ice cover deformation is sampled by RGPS grid cells with dimensions of approximately 10 km on a side. In this paper, we provide a survey of the evolution of these features over a six-month period between November 1996 and April 1997.

1. INTRODUCTION

Modeling of sea ice is based on the principles of conservation of mass and momentum, and requires knowledge of various forces acting on the ice floes. These include the Coriolis force, water drag, air drag, gradients due to the tilt of the sea surface, and the internal ice stresses resulting from floe-to-floe interactions. In the Arctic Ocean, where sea ice motion is constrained by continental boundaries, strong interactions between ice floes take place and influence the basin-wide circulation and deformation of the ice cover. Mechanical deformation results in divergence, convergence, and shear of the ice pack. The opening of cracks in the ice create areas of open water and significantly affect air-ice-ocean interaction. In winter, newly opened leads are the source of new ice growth, brine rejection to the ocean, and rapid heat transfer from the ocean to the atmosphere. Areas of open water and thin

ice dominate the net heat flux into the atmosphere and salt flux into the ocean. Closings of the ice cover causes ice to raft and to pile up into pressure ridges and forced down into keels, increasing the ice-ocean and ice-atmosphere drag This interplay of thermodynamics and dynamics maintains the character of the thickness distribution of the Arctic Ocean ice cover.

An accurate ice dynamics model for climate studies must reflect the appropriate proportions of these processes as well as their beginning and end states. Each of these processes alters the sea ice thickness distribution in a unique manner. Prior to the availability of kinematics data from the SAR, there exists very little data that allows the characterization of the spatial distribution and temporal development of these linear features. Estimates of open water concentrations [*Cavalieri et al.*, 1984] in the Arctic Ocean have been routinely derived from low-resolution passive microwave observations (SMMR and SSM/I), and lead statistics and thin ice thickness have been derived from AVHRR data [*Lindsay and Rothrock*, 1995; *Yu and Rothrock*, 1996]. These studies have focused on the understanding of the effects of leads on the net radiative flux. Using several NOAA-2 images and higher-resolution Landsat imagery, *Marko and Thomson* [1977] and *Erlingsson* [1988] examined the two dimensional deformation patterns of open leads in sea ice and pointed out that slip lines would exhibit linear patterns based on Mohr-Coulomb yield criterion. The other mechanical responses (ridging/rafting, shear) of the ice cover are typically neglected due to the resolution of the sensors.

In recent years, the availability of small volumes of ice motion data from high-resolution SAR data has allowed a more detailed look at the deformation of the ice cover. *Fily and Rothrock* [1990] examined digital methods to determine the linear openings and closings in the ice cover. *Stern et al.* [1994] studied the parameterization of open water production based on area-averaged deformation. They showed that the small-scale (several kilometer) lead activity can be parameterized fairly well in terms of the large scale (several hundred kilometer) strain invariants. *Cunningham et al.* [1994] measured the orientation of newly-opened leads in a small numher of SAR images. *Overland et al.* [1998] used SAR ice motion to examine the granular-plastic properties of sea ice and reviewed the history of leads and their interpretations. The LKFs observed in these studies are clearly related to past ice deformation and their patterns and orientation are related to the constitutive behavior of the ice pack and the way the pack interacts with the coast. However, there is certainly nothing that we could hold out as a climatology of LKF properties.

Linear Kinematic Features (LKFs) refer to the long, narrow features that could contain open water, new ice, nilas, young-ice, first-year ice, rafted ice, or ridged ice. They can be created by divergence, convergence, shear, or a combination of these processes. We choose this more descriptive term because we feel that 'leads' are too restrictive as they refer only to water-filled openings in the ice cover. The characteristics of the LKFs are significant for the rheological behavior of the ice pack and the crucial climate-related processes associated with them (heat flux, salt flux, ridging/rafting). In this paper, we provide a survey of these features, as observed in the RGPS data set, over a n-month period between November 1996 and April 1997.

2. RGPS DATA SET

The RADARSAT Geophysical Processor System (RGPS) tracks Lagrangian elements (cells) of sea ice in SAR imagery over time, thus allowing us to following their location and deformation history [*Kwok et al.*, 1995; *Kwok*, 1998]. Beginning in November of 1996 and continuing today, 3-day SAR maps of the western Arctic Ocean within the Alaska SAR Facility (ASF) Reception mask in Fairbanks, Alaska are being acquired. These maps are used as inputs to the RGPS, a data system that processes the sequential SAR maps into basin-wide fields of ice motion and deformation, and estimates of ice age and thickness. From the RGPS products, we have near 3-day repeat observations of the motion and deformation of each cell.

The RGPS tracking scheme for the 1996/97 winter was initialized on November 4, 1996 by covering the entire Arctic Ocean with a matrix of 10 km by 10 km cells. Coastal regions (within 100 km) are sampled by 25 km by 25 km cells as tracking ice features in these areas is more difficult. In Fig. 1, we show the sequence of divergence, vorticity, shear, and motion of the cell population over the 6-month period between November 1996 and April 1997. In order to show the deformation of the entire period, we plot only the average daily divergence, vorticity, shear, and motion over six-day intervals, instead of at the RGPS sampling interval of three days. The initial grid shown in the Fig. 1 covers an area of $\sim 2.52 \times 10^6$ km^2 (covered by more than 25,000 cells). At the end of April, this region covers $\sim 2.59 \times 10^6$ km^2, a divergence of ~3%.

3. A SURVEY - NOVEMBER 1996 THROUGH APRIL 1997

Here, we provide a broad survey of the LKFs in the RGPS data in terms of their character of deformation, their activity and persistence, and their orientation and length scale.

3.1 DEFORMATION

Here, we compute divergence, vorticity, and shear via:

$$\nabla \cdot u = \tfrac{1}{2}(u_x + v_y), \quad \zeta = \tfrac{1}{2}(v_x - u_y) \quad , e = \left[(u_x - v_y)^2 + (u_y + v_x)^2\right]^{\frac{1}{2}}$$

u_x, u_y, v_x, v_y are the spatial gradients in ice motion computed using a contour integral around the boundary of the cell. $\nabla \cdot u$ is a measure of area change, ζ is the principle measure of rotation, and e is the scalar magnitude of shear. There are a total of thirty fields of divergence, vorticity, shear, and magnitude of motion over the 6-month period. Isobars of 6-day average sea-level pressure (contour interval: 2 hPa) are superimposed on the motion fields. Geostrophic wind direction is parallel to the contour lines and ice motion is to the right but near parallel to the wind.

Between November 10 and November 16, the four fields of deformation and motion show distinctive patterns of LKFs over the ice cover. The pixel color represents the magnitude of that quantity computed at each RGPS cell. All deformation are localized along these features while large regions of the ice cover remain rigid (yellow), with little or no deformation and area change. The LKFs in the regions of divergence north of the Alaskan coast and convergence west of the Canadian archipelago are obscured because of the density of the LKFs. There seem

to be two dominant systems of LKFs at an angle to each other. Within each system the LKFs are near parallel to each other. The lengths of some of these features are quite remarkable, several can be seen to span a large fraction of the Arctic Ocean.

The association between divergence, vorticity, and shear is interesting. First, we note a special property of ζ - a cell in simple shear can induce a positive or negative vorticity, as illustrated in Fig. 2, without actual angular rotation. For example, if two rigid floes slide against each other with no area change (slip line), then the sign of ζ provides an indication of the sense of relative motion of the floes defined by the 'handedness' of the coordinate-system. The average vorticity field of November 10 through November 16 shows regions of clockwise rotation as well as the sense of motion between near rigid elements of the ice cover. The parallel LKFs in each system have the same sense i.e. motion of the rigid plates relative to each other. Divergence and convergence are not always associated with the quasi-linear patterns of shear sampled by the RGPS cells.

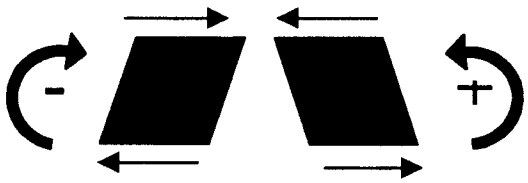

Figure 2. Vorticity and simple shear.

The cumulative deformation of the ice cover over the 6-month period as sampled by the RGPS cells is shown in Fig. 3. The total deformation of each cell on April 30, 1997 is computed by first summing the velocity gradients over the period and then calculating the divergence, vorticity, and shear of the cell. These fields provide a broad summary of the spatial distribution of deformation of the ice cover over six months. Most of the divergent cells are located south of 80°N in the Beaufort and Chukchi Seas. The cumulative divergence of the cells in the central Arctic, north of 80°N, is smaller except for the activity of the cells west of the Canadian archipelago and north of the Greenland coast. The vorticity map shows a coherent rotation (anticyclonic) of the sea ice cover north of the Alaska coast that is an expression of the Beaufort Gyre. Over the 6 months, the net rotation of this region is over 100°. The remainder of the map shows translational motion. The shear field shows that the largest shear are localized along linear features which are indicative of lead openings, ridging events or slip lines on the ice cover. There are high concentrations of these in the lower latitudes close to the Alaska and Siberian coasts. The LKFs separate distinct areas characterized by very little deformation.

3.2 ACTIVITY

We define activity as the relative abundance of LKFs within the area of interest. The density of the isobars indicates the strength of wind-forcing and the response of the ice cover can be seen in the activity of LKFs and intensity of the motion fields. In November and December, the motion fields show that almost the entire ice cover moves in response to the large-scale atmospheric forcing. After early January, the response to atmospheric forcing is attenuated with only regional motion patterns

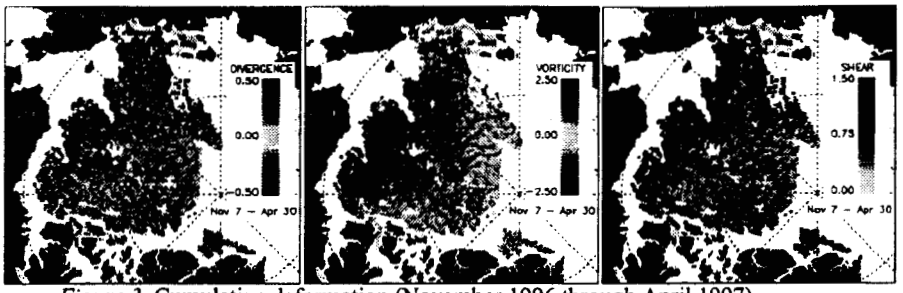

Figure 3. Cumulative deformation (November 1996 through April 1997).

associated with relatively high winds. Several periods (Jan 3-9, Feb 2-8, Feb 20-26, Mar 22-28, Mar 28-Apr 3) show very little motion and a correspondingly lower density of LKFs. Over the winter months, consolidation and thickening of the ice cover contribute to an overall increase in ice strength and a decrease in deformation. The abundance of the LKFs are correlated to motion gradient. LKF activity decreases after Jan 3. The period between Mar 16 and Mar 28 has the lowest activity over the 6 months. This is followed by an increase in LKF activity beginning around mid-to-late April when the activity resembles more of that observed in November than in January, February, and March - perhaps an indication of the onset of spring melt.

3.3 PERSISTENCE

Persistence in the LKF patterns can be seen in the sequence of deformation fields. We refer to persistence as the length of time a system of LKFs with the same approximate orientation remains active. A system of LKFs would remain active if similar external forcing (wind direction) persists or because of preferential failure of weaker ice along these feature. When an LKF, or a system of nearly parallel LKFs exists in a region, the ice obviously retains its strength parallel to the LKF direction while having weaker strength across it. These systems of LKFs, which may span the entire basin, determine the subsequent mechanical behavior of the ice cover to external forcing. Since the ice is weaker along these features, the ice cover becomes anisotropic, and its mechanical properties are no longer identical in all directions. Mechanical behavior of the ice cover to external forcing would be dependent on the development of these features. As the ice in these features thickens and deforms, the ice will eventually attain the strength of thicker ice and changes in external forcing would introduce a different system of LKFs.

Visually, one could roughly see five different prevailing patterns of LKFs over the ice cover with each spanning the following periods: Nov 10-Dec 10, Dec 10-Jan 9, Jan 9-Feb 28, Feb 28-April 3, and Apr 3-May 9. Within each period of approximately a month the LKF patterns remain relatively unchanged even though the wind-forcing, as indicated by the pressure contours, are highly variable. On occasions, typically during the transition from one set of LKF patterns to another, the LKFs are aligned with the isobars. For the sea ice in the old system of LKF, it could represent an increase in ice strength such that it is no longer as likely to fail. The onset of a new pattern of LKFs is an interesting topic of study.

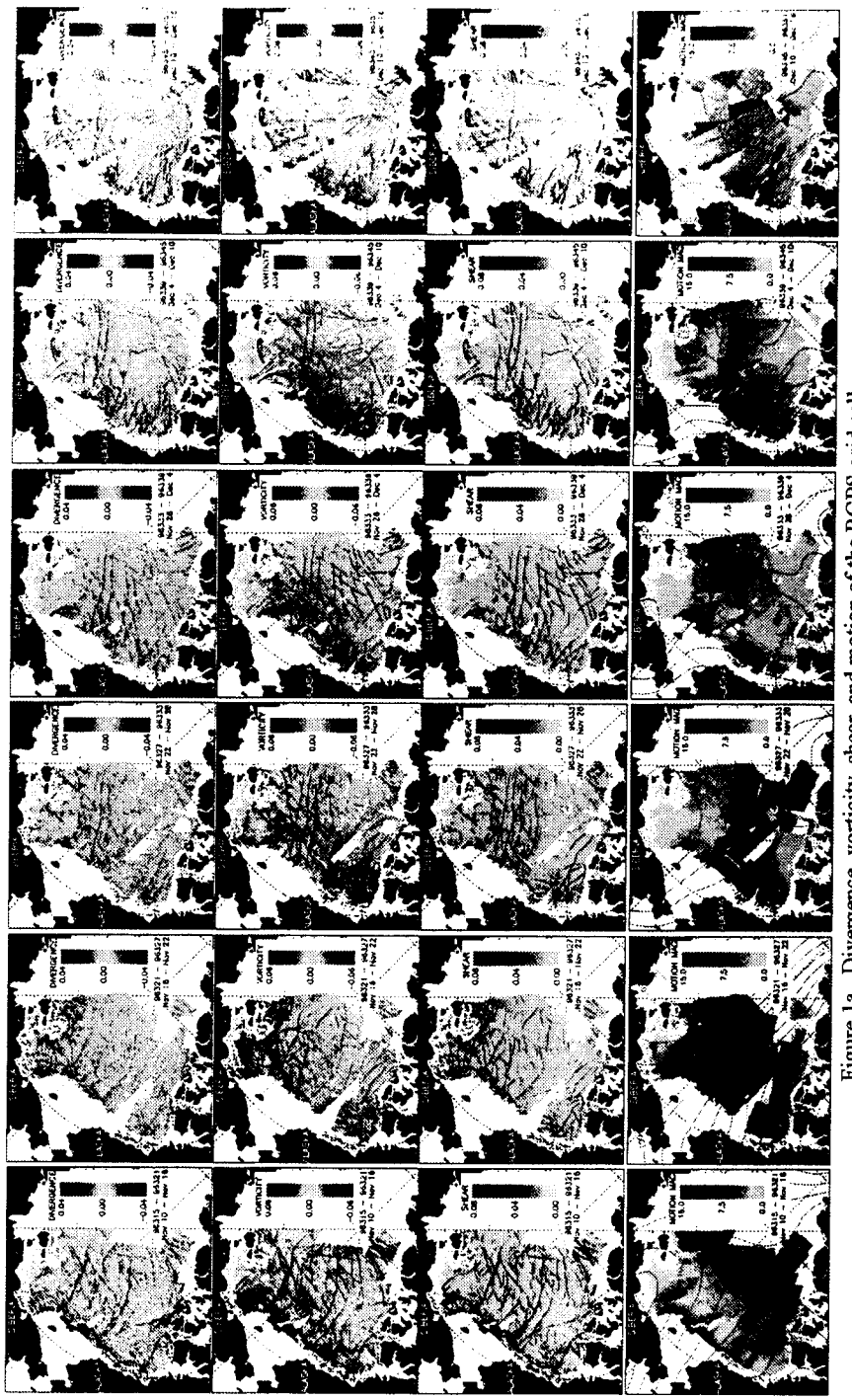

Figure 1a. Divergence, vorticity, shear, and motion of the RGPS grid cells.

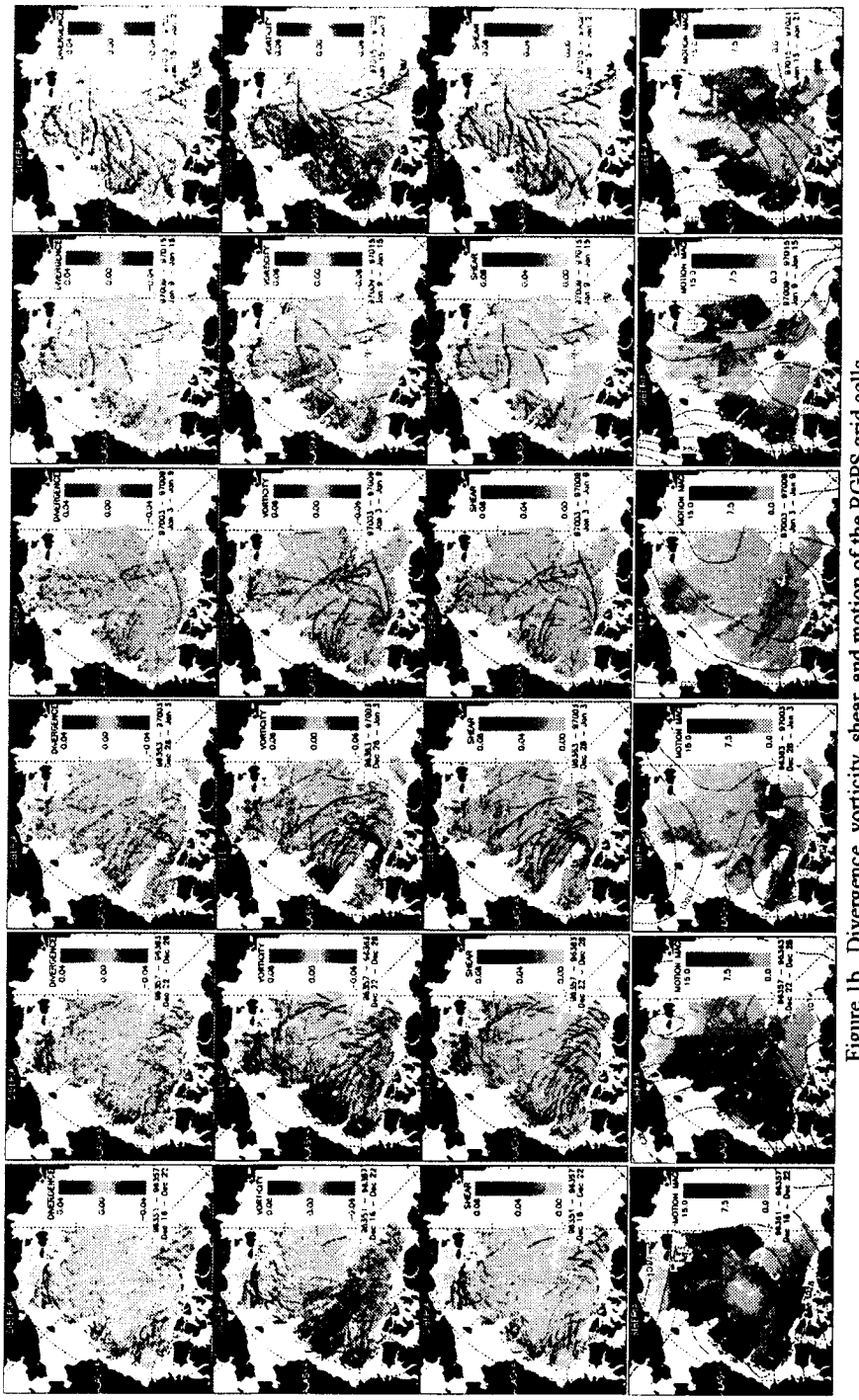

Figure 1b. Divergence, vorticity, shear, and motion of the RGPS grid cells.

igure 1c. Divergence, vorticity, shear, and motion of the RGPS grid cells.

Figure 1d. Divergence, vorticity, shear, and motion of the RGPS grid cells.

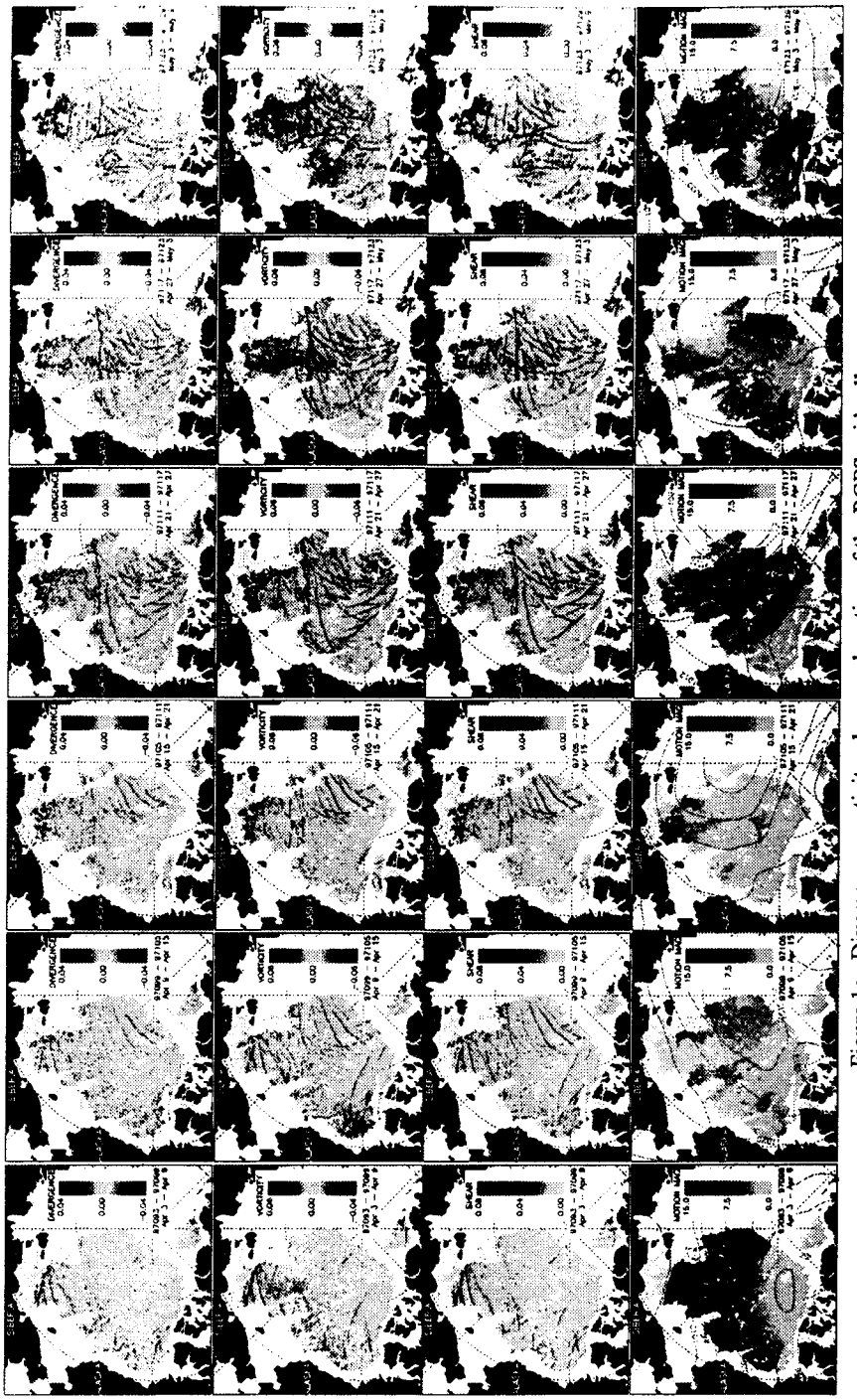

Figure 1e. Divergence, vorticity, shear, and motion of the RGPS grid cells.

3.4 ORIENTATION/LENGTH SCALE

In addition to the persistence of the systems of LKFs, their orientations are important in the context of material properties, external forcing, and boundary conditions. The current generation of models assumes the sea ice to be an isotropic viscous-plastic material. Over large length scales, say several hundred kilometers, it is often assumed that as more leads of random orientation appear in each neighborhood, the behavior can be approximated as isotropic. However it is evident from the RGPS observations (Fig. 1) that at the length scales observed in the RGPS data set, LKFs form oriented, organized, and persistent patterns. When an LKF is present, it has weaker strength across it, yet it retains its strength along its length. The dynamical behavior of this strongly oriented, or anisotropic, material must differ in these directions [*Coon*, 1998]. Thus, pack ice is an anisotropic material for most of the year, with the ice dynamics affected by LKFs which appear as velocity discontinuities or slip lines in RGPS ice motion products.

The relative orientation of intersecting LKFs has been a topic of interest due to the implied stress field and material behavior of sea ice. We simply note here that LKFs intersecting at acute angles forming diamond patterns can be observed in the RGPS data. These intersecting patterns stand out during these periods: Nov 10-Nov 16, Nov 28-Dec 4, Jan 15-Jan 21, Apr 21-Apr 27, Apr 27-May 3, and May 3-May 9. The dense patterns of LKFs just north of the Alaskan coast are also interesting but are obscured due to the resolution of the plots here.

4. SUMMARY

This present survey of sea ice cover deformation is qualitative in nature. Nevertheless, it demonstrates that the RGPS products provide an unprecedented level of spatial and temporal detail of the deformational processes over the six months between November 1996 through April 1997. We can observe the temporal development of basin-wide LKFs in all its forms i.e. opening, closing, and shear. Their activity, persistence, orientation, and the length scale of the LKFs over the six-month period are remarkable and interesting. This is one step toward a more detailed understanding of the large scale expressions of the deformation of the ice cover.

With the advent of high resolution coupled ice-ocean models (e.g. *Zhang et al.* [1999], *Zhang et al.* [1998]) that approaches the widths of leads, the distinction between isotropy and anisotropy has become even more significant. The consequence of an anisotropic ice cover is not well-understood in terms of the modeled surface heat and mass balance. The RGPS data set is a crucial component in the testing of new models that accounts for the spatial and temporal characteristics of the linear kinematic features observed here.

Acknowledgement

The RADARSAT imagery are processed and calibrated at the Alaska SAR Facility, Fairbanks, AK. The RGPS is a joint project of the Alaska SAR Facility and the Jet Propulsion Laboratory. R. Kwok performed this work at the Jet Propulsion

Laboratory, California Institute of Technology under contract with the National Aeronautics and Space Administration.

References

Cavalieri, D. J., P. Gloersen, and W. J. Campbell, Determination of sea ice parameters from Nimbus 7 SMMR, *J. Geophys. Res.*, 89(D4), 5355-5369, 1984.

Coon, M. D., G. S. Knoke, D. C. Echert, and R. S. Pritchard, The architecture of an anisotropic elastic-plastic sea ice mechanics constitutive law, *J. Geophys. Res.*,103(C10), 21915-21925, 1998.

Cunningham, G. F., R. Kwok, and J. Banfield, Ice lead orientation characteristics in the winter Beaufort Sea. *Proceedings of IGARSS*, Pasadena, CA 1994.

Erlingsson, B., Two-dimensional deformation patterns in sea ice, *J. Glacio.*, 34(118), 301-308, 1988. Hopkins, M. A., J. Tuhkuri, and M. Lensu, Rafting and ridging of ice sheets, *J. Geophys. Res.*, 104 (C6), 13605-13613, 1999.

Kwok, R., D. A. Rothrock, H. L. Stern and G. F. Cunningham, Determination of Ice Age using Lagrangian Observations of Ice Motion, *IEEE Trans. Geosci. Remote Sens.*, 33(2), 392-400, 1995.

Kwok, R., The RADARSAT Geophysical Processor System, in: *Analysis of SAR data of the Polar Oceans*, C. Tsatsoulis and R. Kwok, eds., Springer-Verlag, Berlin, 235-257, 1998.

Li, S., Z. Cheng, W. F. Weeks, A grid based algorithm for the extraction of intermediate-scale sea ice deformation descriptors from SAR ice motion products, *Int. J. Remote Sens.*, 16 (17), 3267-3286, 1995.

Lindsay, R. W. and D. A. Rothrock, Arctic sea ice leads from advanced very high resolution radiometer images, *J. Geophys. Res.*, 100(C3), 4533-4544, 1995

Lindsay, R., H. Stern, D. A. Rothrock, Y. Yu, and R. Kwok, Validation of RADARSAT Geophysical Processor System Products, (http:://psc.washington.edu/), 2000.

Marko, J. R., and R. E. Thomson, Rectilinear leads and internal motions in the ice pack of the western Arctic Ocean, *J. Geophys. Res.*,82(6), 979-987, 1977.

Overland, J. E., S. L McNutt., S. Salo, J. Groves and S. S. Li, Arctic sea ice as a granular plastic, *J. Geophys. Res.*, 103 (C10), 21845-21867, 1998.

Stern, H. L., D. A. Rothrock and R. Kwok, Open Water Production in Arctic Sea Ice: Satellite measurements and model parameterizations, *J. Geophys. Res.*, 100 (C10), 20601-20612, 1995.

Yu,, Y, and D. A. Rothrock, Thin ice thickness from satellite thermal imagery, *J. Geophys. Res.*, 101(C10), 25753-25766,1966.

Zhang, Y., Maslowski, W., and Semptner, A. J., Impact od mesoscale ocean currents on sea ice in high-resolution Arctic ice and ocean simulations, *J. Geophys. Res.*, 104(C8), 18,409-18,430, 1999.

Zhang, J., W. Hibler, M. Steele, and D. Rothrock, Arctic ice-ocean modeling with and without climate restoring, *J. Phys. Oceanogr., 28,* 191-217, 1998.